STRUCTURAL CHEMISTRY

ISSN: 2053-2296
journals.iucr.org/c

Crystal structures of two (5,5,7,12,12,14-hexamethyl-1,4,8,11-tetraazacyclotetradecane)iron(III) complexes

Reese A. Clendening, Matthias Zeller and Tong Ren

Acta Cryst. (2019). C**75**, 1509–1516

Acta Cryst C STRUCTURAL CHEMISTRY
ISSN 2053-2296

Crystal structures of two (5,5,7,12,12,14-hexamethyl-1,4,8,11-tetraazacyclotetradecane)iron(III) complexes

Reese A. Clendening, Matthias Zeller* and Tong Ren*

Department of Chemistry, Purdue University, 560 Oval Dr., W. Lafayette, IN 47907-2084, USA. *Correspondence e-mail: zeller4@purdue.edu, tren@purdue.edu

Received 16 August 2019
Accepted 11 October 2019

Edited by E. Y. Cheung, Amgen Inc., USA

Keywords: iron(III); tetraazacyclotetradecane; crystal structure; *cis* configuration; *trans* configuration.

CCDC references: 1958894; 1958895

Supporting information: this article has supporting information at journals.iucr.org/c

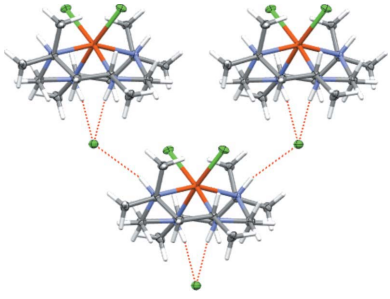

Reported in this contribution are the synthesis and crystal structures of two new Fe^{III} complexes of 5,5,7,12,12,14-hexamethyl-1,4,8,11-tetraazacyclotetradecane (HMC), namely, dichlorido(5,5,7,12,12,14-hexamethyl-1,4,8,11-tetraazacyclotetradecane)iron(III) chloride, $[FeCl_2(C_{16}H_{36}N_4)]Cl$ or *cis*-$[FeCl_2(rac\text{-HMC})]Cl$ (**1**), and dichlorido(5,5,7,12,12,14-hexamethyl-1,4,8,11-tetraazacyclotetradecane)-iron(III) tetrachloridoferrate, $[FeCl_2(C_{16}H_{36}N_4)][FeCl_4]$ or *trans*-$[FeCl_2(meso\text{-HMC})][FeCl_4]$ (**2**). Single-crystal X-ray diffraction studies revealed that both **1** and **2** adopt a pseudo-octahedral geometry, where the macrocycles adopt folded and planar geometries, respectively. The chloride ligands in **1** are *cis* to each other, while those in **2** have a *trans* configuration. The relevant bond angles in **1** deviate substantially from an ideal octahedral coordination geometry, with the angles between the *cis* substituents varying from 81.55 (5) to 107.56 (4)°, and those between the *trans*-ligating atoms varying from 157.76 (8) to 170.88 (3)°. In contrast, **2** adopts a less strained configuration, in which the N—Fe—N angles vary from 84.61 (8) to 95.39 (8)° and the N—Fe—Cl angles vary from 86.02 (5) to 93.98 (5)°.

1. Introduction

There has been recent interest in developing conjugated materials based on alkynyl complexes of 3*d* metals with cyclam (1,4,8,11-tetraazacyclotetradecane) or its *C*-functionalized derivatives as the supporting ligand (Ren, 2016). Noteworthy examples include magnetic coupling between Cr(cyclam) species mediated by ethynyltetrathiafulvalene ligands (Nishijo *et al.*, 2011), the formation of $[Co(cyclam)Cl]_2(\mu\text{-}C_{2m})$ (m = 2–6) series (Cook *et al.*, 2015, 2016) and Co-based cross-conjugated *gem*-DEE complexes (*gem*-DEE is *gem*-diethynylethene; Natoli *et al.*, 2015, 2016, 2019), and phosphorescence from $[Cr(cyclam')(C_2R)_2]$-type complexes, with cyclam′ as either 5,5,7,12,12,14-hexamethyl-1,4,8,11-tetraazacyclotetradecane (HMC; Tyler *et al.*, 2016) or 5,12-dimethyl-1,4,8,11-tetraazacyclotetradecane (DMC; Judkins *et al.*, 2017). In particular, several *trans*-$[Fe(cyclam)(C_2R)_2]$-type complexes were prepared by the reactions between LiC_2R and $[FeCl_2(cyclam)]Cl$ (Cao *et al.*, 2012, 2013). Interestingly, there was no evidence of the formation of *cis*-$[Fe(cyclam)(C_2R)_2]$, despite the fact that the $[FeCl_2(cyclam)]Cl$ starting material comprises both *cis* (predominant) and *trans* (minor) isomers. Encouraged by the clean preparation of both *trans*-$[Cr(meso\text{-HMC})(C_2R)_2]^+$ and *cis*-$[Cr(rac\text{-HMC})(C_2R)_2]^+$, we are pursuing the elusive *cis*-Fe alkynyl complex using HMC as the supporting tetraaza ligand. Described in this article are the preparation of *cis*-$[FeCl_2(rac\text{-HMC})]Cl$ (**1**) and *trans*-$[FeCl_2(meso\text{-HMC})][FeCl_4]$ (**2**) from pure *meso*- and *rac*-HMC, respectively, and the structural characterization of **1** and **2**.

Table 1
Experimental details.

Experiments were carried out at 150 K on a Bruker D8 Quest CMOS diffractometer. Absorption was corrected for by multi-scan methods (Krause *et al.*, 2015). H atoms were treated by a mixture of independent and constrained refinement.

	(1)	(2)
Crystal data		
Chemical formula	$[FeCl_2(C_{16}H_{36}N_4)]Cl$	$[FeCl_2(C_{16}H_{36}N_4)][FeCl_4]$
M_r	446.69	608.89
Crystal system, space group	Orthorhombic, *Fdd*2	Monoclinic, $P2_1/c$
a, *b*, *c* (Å)	34.5658 (16), 9.3832 (4), 12.5209 (6)	6.5569 (2), 19.1663 (5), 20.2946 (5)
α, β, γ (°)	90, 90, 90	90, 95.3558 (15), 90
V (Å^3)	4061.0 (3)	2539.32 (12)
Z	8	4
Radiation type	Mo *K*α	Cu *K*α
μ (mm^{-1})	1.14	15.06
Crystal size (mm)	0.18 × 0.17 × 0.05	0.18 × 0.09 × 0.05
Data collection		
T_{min}, T_{max}	0.595, 0.747	0.426, 0.754
No. of measured, independent and observed [$I > 2\sigma(I)$] reflections	17097, 4166, 3897	26483, 5481, 4930
R_{int}	0.042	0.044
(sin $\theta/\lambda)_{max}$ (Å^{-1})	0.795	0.641
Refinement		
$R[F^2 > 2\sigma(F^2)]$, $wR(F^2)$, *S*	0.025, 0.064, 1.06	0.032, 0.086, 1.11
No. of reflections	4166	5481
No. of parameters	120	274
No. of restraints	2	6
$\Delta\rho_{max}$, $\Delta\rho_{min}$ (e Å^{-3})	0.86, −0.58	0.76, −0.57
Absolute structure	Refined as an inversion twin	–
Absolute structure parameter	0.004 (13)	–

Computer programs: *APEX3* (Bruker, 2018), *SAINT* (Bruker, 2018), *SHELXM* (Sheldrick, 2008), *SHELXL2018* (Sheldrick, 2015), *SHELXLE* (Hübschle *et al.*, 2011), *Mercury* (Macrae *et al.*, 2008) and *publCIF* (Westrip, 2010).

2. Experimental

Both *meso*- and *rac*-HMC were prepared according the procedure of Hay *et al.* (1975). The syntheses of both *cis*-$[FeCl_2$(*rac*-HMC)]Cl (**1**) and *trans*-$[FeCl_2$(*meso*-HMC)]$[FeCl_4]$ (**2**) were accomplished using a procedure modified from that used for $FeCl_2$(*rac*-HMC) by Dei *et al.* (1993), as detailed below.

2.1. Synthesis and crystallization

2.1.1. Preparation of *cis*-[$FeCl_2$(*rac*-HMC)]Cl (1). $FeCl_2{\cdot}4H_2O$ (0.36 g, 1.8 mmol) was dissolved in a degassed solution (15 ml) of dimethyformamide–triethyl orthoformate (2:1 *v*/*v*). This solution was refluxed under nitrogen for 30 min, during which time the solution darkened in color. Similarly, *rac*-HMC (0.50 g, 1.76 mmol) was dissolved in a 3:1 (*v*/*v*) mixture (20 ml) of dimethylformamide and triethyl orthoformate. This solution was purged with nitrogen and heated to reflux under nitrogen. The two solutions were then combined and allowed to stir at 100 °C under nitrogen for 45 min. Hydrochloric acid (0.4 ml of 12 *N* HCl, 4.8 mmol) was added dropwise, causing the solution to fume and turn yellow. Oxygen was bubbled through the solution for 1 h, resulting in a rapid color change to dark orange. The solution was filtered to yield the product as a yellow–orange solid. Additional solid was obtained upon removal of the solvent *in vacuo via* an external trap followed by filtration and washing with acetone and minimal methanol. The product was crudely purified by extraction with methanol. Crystals suitable for analysis were grown by slow diffusion of acetone into a concentrated aqueous solution of the product (yield 31%). ESI–MS (*m*/*z*): 410 [M^+]. IR (cm^{-1}): N—H 3157 (*m*) and 2671 (*m*). UV–Vis spectra, λ [nm, ε, (M^{-1} cm^{-1})]: 318 (2, 900) (*sh*). μ_{eff} = 5.90 μ_B. M.p. 234 °C (decomposition).

2.1.2. Preparation of *trans*-[$FeCl_2$(*meso*-HMC)]$[FeCl_4]$ (2). A 2:1 (*v*/*v*) mixture of methanol and triethyl orthoformate (40 ml) was purged with nitrogen prior to the addition of $FeCl_2{\cdot}4H_2O$ (0.52 g, 2.6 mmol). Similarly, *meso*-HMC (0.25 g, 0.88 mmol) was dissolved in the same solvent mixture (20 ml). This solution was also purged with nitrogen. Both solutions were heated to reflux under nitrogen for 1.3 h. The iron solution was transferred *via* cannula to the *meso*-HMC solution. The resulting solution was heated at 80 °C under nitrogen for 1.5 h. Oxygen was then passed through the solution for 1.5 h. Concentrated hydrochloric acid (0.50 ml, 6 mmol HCl) was added and oxygen continued to be passed through the solution for another 1.5 h. After the solution had been allowed to stand at room temperature undisturbed for 2 h, the product was filtered off and washed with diethyl ether. The product may be purified by recrystallization from acetone. Crystals suitable for X-ray diffraction were grown by the slow diffusion of diethyl ether into a concentrated solution of the crude product in a dichloromethane/methanol mixture (yield 0.224 g, 42%). ESI–MS (*m*/*z*): 410 [M^+]; negative: 198 [$FeCl_4^-$]. IR (cm^{-1}): N—H 3201 (*m*). UV–Vis spectra, λ [nm,

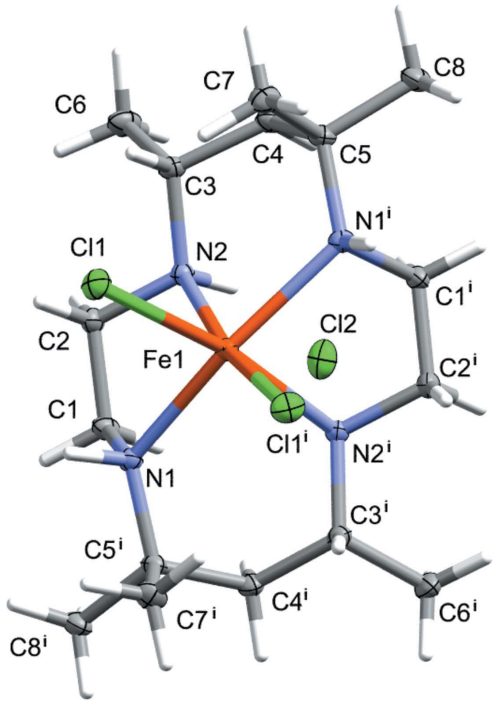

Figure 1
Displacement ellipsoid plot (50% probability level) of **1**. H-atom labels have been omitted for clarity. [Symmetry code: (i) $-x, -y+1, z$.]

ε, (M^{-1} cm^{-1})]: 291 (3, 990) (*sh*), 526 (127) (*sh*). μ_{eff} = 7.08 μ_B. M.p. 188 °C (decomposition).

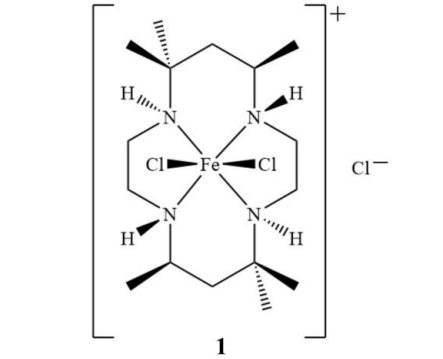

1

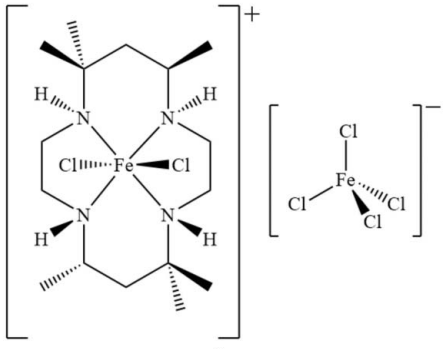

2

2.2. Refinement

Compound **1** was refined as an inversion twin [BASF = 0.005 (13)]. In both **1** and **2**, all H atoms were placed in calculated positions and constrained to ride on their parent atoms. CH, CH_2, and CH_3 C—H bond lengths were constrained to 1.00, 0.99, and 0.98 Å, respectively. The positions of the amine H atoms were refined, but within each structure, the N—H distances were restrained to be similar to each other, with an s.u. value of 0.02 Å. Methyl groups were permitted to rotate. Isotropic U values for H atoms were set to a multiple of U_{eq} of the parent atom (1.5 for CH_3, and 1.2 for all other C—H and N—H hydrogens). Experimental details and crystal data are given in Table 1.

Table 2
Selected geometric parameters (Å, °) for **1**.

Fe1—N2	2.2081 (14)	Fe1—N1^{i}	2.2150 (14)
Fe1—N1	2.2149 (14)	Fe1—Cl1	2.3065 (5)
N2—Fe1—N2^{i}	92.75 (7)	N1—Fe1—Cl1	88.06 (4)
N2—Fe1—N1	81.55 (5)	N2—Fe1—Cl1^{i}	170.88 (3)
N2—Fe1—N1^{i}	83.15 (5)	N1—Fe1—Cl1^{i}	107.56 (4)
N1—Fe1—N1^{i}	157.76 (8)	Cl1—Fe1—Cl1^{i}	92.01 (2)
N2—Fe1—Cl1	88.35 (4)		

Symmetry code: (i) $-x, -y+1, z$.

Table 3
Selected geometric parameters (Å, °) for **2**.

Fe1—N1	2.0768 (19)	Fe2—Cl2	2.2760 (5)
Fe1—N2	2.0477 (19)	Fe3—Cl3	2.1866 (8)
Fe2—N3	2.0595 (19)	Fe3—Cl4	2.2117 (8)
Fe2—N4	2.0301 (18)	Fe3—Cl5	2.1879 (7)
Fe1—Cl1	2.3177 (5)	Fe3—Cl6	2.2048 (8)
N2—Fe1—N1^{i}	84.61 (8)	N3—Fe2—Cl2	86.49 (5)
N2—Fe1—N1	95.39 (8)	N4—Fe2—Cl2^{ii}	92.23 (5)
N2—Fe1—Cl1	91.68 (5)	N3—Fe2—Cl2^{ii}	93.51 (5)
N1—Fe1—Cl1	93.98 (5)	Cl3—Fe3—Cl5	109.53 (3)
N2—Fe1—Cl1^{i}	88.32 (5)	Cl3—Fe3—Cl6	108.24 (4)
N1—Fe1—Cl1^{i}	86.02 (5)	Cl5—Fe3—Cl6	110.05 (3)
N4—Fe2—N3	95.04 (7)	Cl3—Fe3—Cl4	108.22 (3)
N4—Fe2—N3^{ii}	84.96 (7)	Cl5—Fe3—Cl4	111.14 (3)
N4—Fe2—Cl2	87.76 (5)	Cl6—Fe3—Cl4	109.60 (3)

Symmetry codes: (i) $-x, -y+2, -z$; (ii) $-x+1, -y+1, -z$.

3. Results and discussion

Compound **1** (see Fig. 1) crystallizes in the space group *Fdd*2 with one formula unit consisting of a chloride anion and the macrocyclic cation. One half of the macrocycle is crystallographically independent and the other half is created by a twofold rotational axis. The outer-sphere chloride ion is also located on a twofold axis. The resulting full molecular formula is $FeC_{16}H_{34}N_4Cl_2{\cdot}Cl$, consistent with an Fe^{III} metal center. See Table 2 for selected geometric parameters.

Compound **2** (see Fig. 2) crystallizes in the space group $P2_1/c$, with three crystallographically independent moieties, *i.e.* two cations and one anion. Again, one-half of each cationic fragment is unique and related to the other half by crystallographic symmetry, here an inversion operation. Although one anionic unit, *i.e.* $[FeCl_4]^-$, is present for each cation, only one such fragment is observed in the asymmetric unit. The formula unit is thus given by $FeC_{16}N_4H_{36}Cl_2{\cdot}FeCl_4$, with each

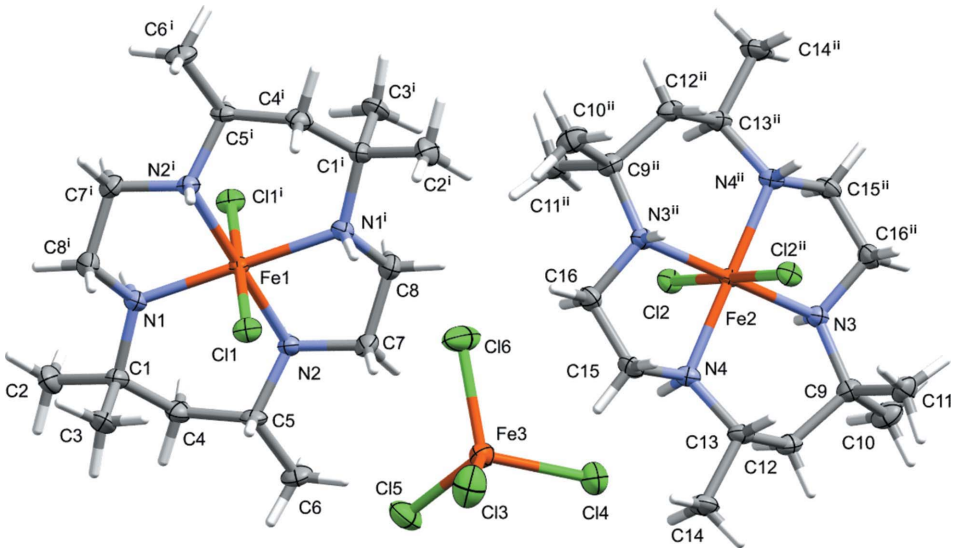

Figure 2
Displacement ellipsoid plot (50% probability level) of **2**. H-atom labels have been omitted for clarity. [Symmetry codes: (i) $-x, -y+2, -z$; (ii) $-x+1, -y+1, -z$.]

iron center in an oxidation state of three. See Table 3 for selected geometric parameters.

Both **1** and **2** exhibit a pseudo-octahedral coordination environment; however, as noted, the details of the coordination spheres differ substantially. In **1**, the macrocycle adopts a *cis*-V (*RRRR*) conformation (Bosnich *et al.*, 1965), leaving two adjacent coordination sites open. This orients the macrocyclic amine groups such that the H atoms of adjacent amine groups face in opposite directions in the complex. This stands in contrast to the orientation of the macrocyclic amine groups in the equatorial plane of **2** (*trans*-III, *RRSS*) (Bosnich *et al.*, 1965), in which the H atoms of adjacent amine groups separated by the $CH_2(CH_3)$–CH_2–$CH_2(CH_3)_2$ bridge face in the same direction, while those separated by the CH_2–CH_2 bridge face in opposite directions. As has been discussed previously (House *et al.*, 1983; Curtis, 1979), the nature of the macrocycle as racemic (in **1**) or *meso* (in **2**) strongly preferences the formation of *cis* or *trans* complexes, respectively.

In **1**, many of the bond angles deviate substantially from the ideal values of 90 and 180°. For example, adjacent N atoms bound to the iron center are separated by angles of 81.55 (5)–83.15 (5)°, with the slightly larger angle belonging to the N atoms separated by the $CH_2(CH_3)$–CH_2–$CH_2(CH_3)_2$ bridge and the smaller angle to those separated by the CH_2–CH_2 bridge. These strained bond angles may be influenced by steric congestion between the chloride ligands and the axial methyl groups (Fig. 3). The axial methyl groups exist necessarily at the dimethyl-substituted portions of the macrocycle (the 5- and 12-positions of 5,5,7,12,12,14-hexamethyl-1,4,8,11-tetraazacyclotetradecane). These positions are adjacent to N1 and N1^{i} (see Table 2) and the influence exerted by these bulky groups is manifest in the N1—Fe—Cl1 bond angle of 107.56 (4)° [*versus* the N2—Fe—Cl1 angle of only 88.35 (4)°] and in the large deviation from linearity along N1—Fe—N1^{i}, *viz.* 157.76 (8)° *versus* the ideal value of 180°. However, a substantial amount of the geometric strain is likely attributable to the *cis* coordination of the macrocycle, as a similar strain has been observed in the related unsubstituted *cis*-

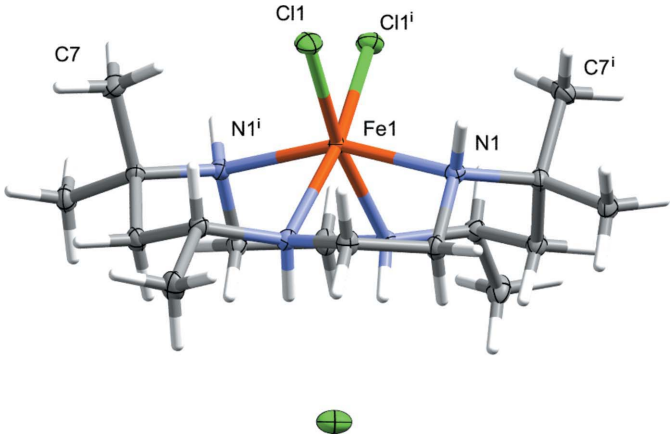

Figure 3
Displacement ellipsoid plot (50% probability level) of the cation of **1**, illustrating the position of the axial methyl groups (C7 and C7^{i}) relative to the chloride ligands (Cl1 and Cl1^{i}). H-atom labels have been omitted for clarity. [Symmetry code: (i) $-x, -y+1, z$.]

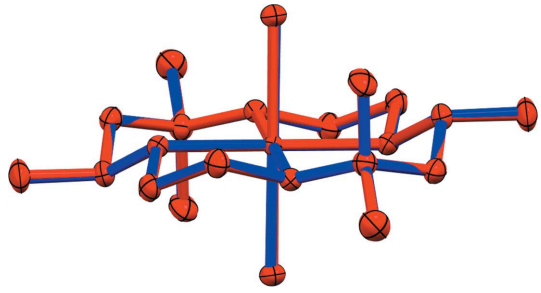

Figure 4
Least-squares overlay of the two crystallographically independent cations in **2** (red and blue; 50% probability displacement ellipsoids).

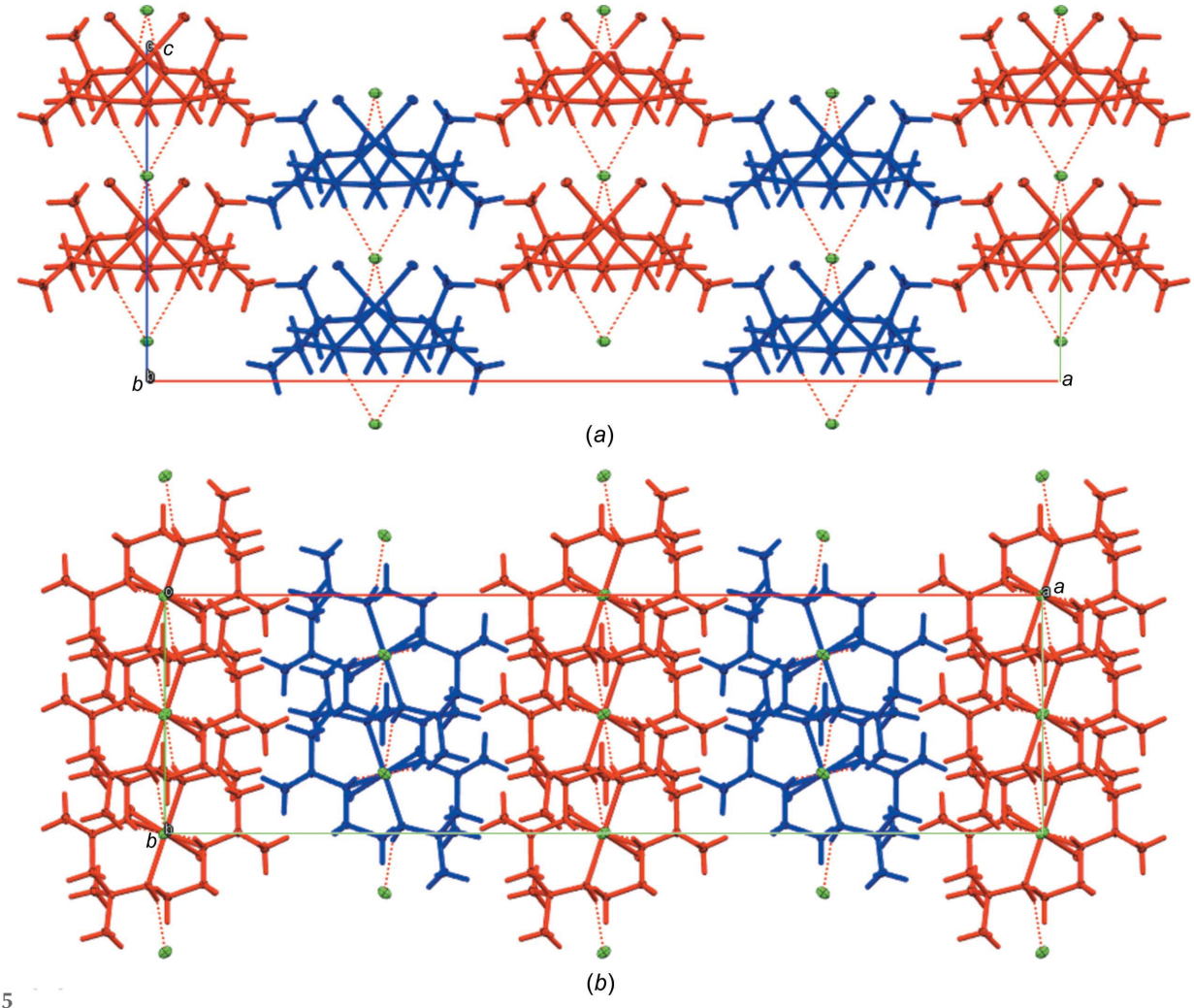

Figure 5
Crystal packing of **1**, viewed along (*a*) the *b* axis and (*b*) the *c* axis. Distinct layers (composed of the two enantiomers) are colored blue and red for clarity. Hydrogen-bonding interactions within each layer are shown as red dotted lines.

Fe^{III}(cyclam) compound (Guilard *et al.*, 1997), which is discussed further below.

Unlike highly strained **1**, the bond angles of the cations in **2** are, on average, much closer to the ideal octahedral geometry. The conformations of the two crystallographically independent cations are also virtually identical (see the least-squares overlay in Fig. 4). Adjacent N atoms are separated by 84.61 (8)–95.39 (8)° in one cation and by 84.97 (7)–95.04 (7)° in the other, with the larger angles in each case once again associated with the N atoms separated by the $CH_2(CH_3)$–CH_2–$CH_2(CH_3)_2$ bridge. The N—Fe—Cl bond angles vary from 86.02 (5) to 93.98 (5)°, with the larger angles seemingly enforced (as in the case of **1**) by the axial methyl groups at the 5- and 12-positions of the macrocycle. Due to the crystallographic inversion symmetry of the cations, all species situated *trans* to each other (across the iron center) exhibit the ideal 180° bond angle. Nonetheless, the bond lengths involving the iron center in both **1** and **2** are quite similar. The Fe—Cl bond lengths average around 2.3 Å. The iron–nitrogen bond lengths in **1** (average 2.21 Å) are somewhat longer than those of **2** (average 2.05 Å). Additionally, the bond lengths and angles of **1** and **2** are quite similar to those of previously reported Fe^{III}(cyclam) complexes, for example, *trans*-

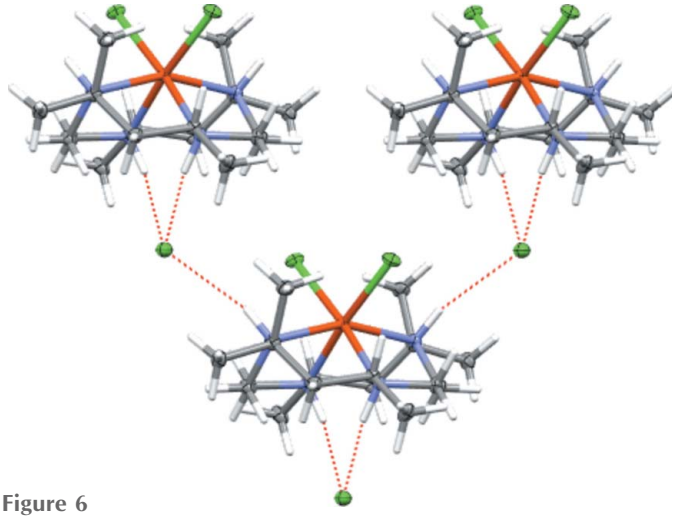

Figure 6
Major hydrogen bonding in **1**. Hydrogen bonds are shown as red dotted lines.

[$FeCl_2$(cyclam)][$FeCl_4$], *cis*-[$FeCl_2$(cyclam)]Cl, and *trans*-[$FeCl_2$(cyclam)]PF_6 (Guilard *et al.*, 1997; Neumann *et al.*, 2003). In all cases, the cationic species show Fe—Cl bond lengths near 2.3 Å (Guilard *et al.*, 1997; Neumann *et al.*, 2003), with slightly shorter bonds in *trans*-[$FeCl_2$(cyclam)]PF_6 of about 2.27 Å (Neumann *et al.*, 2003). For the unsubstituted macrocycle, the bond lengths between the Fe^{III} ions and the N atoms tend to be just slightly shorter than those of **1** and **2**. The *trans* and *cis* forms of the Fe(cyclam) complexes show the same trends in bond angles, with significant strain evident in the *cis* complex, as in **1** (Guilard *et al.*, 1997). However, the steric effect of the methyl substituents is evident in some of the bond angles. In the unsubstituted *cis*-[$FeCl_2$(cyclam)]Cl, the N—Fe—Cl angle varies from approximately 96.5 to 98.4° (Guilard *et al.*, 1997), whereas in **1**, these angles vary from 88.06 (4) to 107.56 (4)°, with the larger angle belonging to the portion adjacent to the axial methyl group, as discussed above. Likewise, in both examples of the *trans*-[$FeCl_2$(cyclam)]$^+$ species, the N—Fe—Cl bond angles vary by only about 3.5° (the total variation for both compounds is approximately 88.2–91.9°) (Guilard *et al.*, 1997; Neumann *et al.*, 2003), whereas in **2**, this variation is approximately 10° (roughly 85–95°), with the larger angles again situated nearest the axial methyl groups. Thus, although it appears that some strain is inherent in the macrocyclic complexes, the methyl substituents of HMC manifest a readily observable steric effect on the geometry of both **1** and **2**.

The intermolecular interactions of **1** (*cis*) are governed by medium-strength hydrogen-bonding-type interactions within distinct regions of the packing. The racemic mixture crystallized with moieties of the same enantiomer related by twofold rotation and screw axes, and with the two enantiomers related

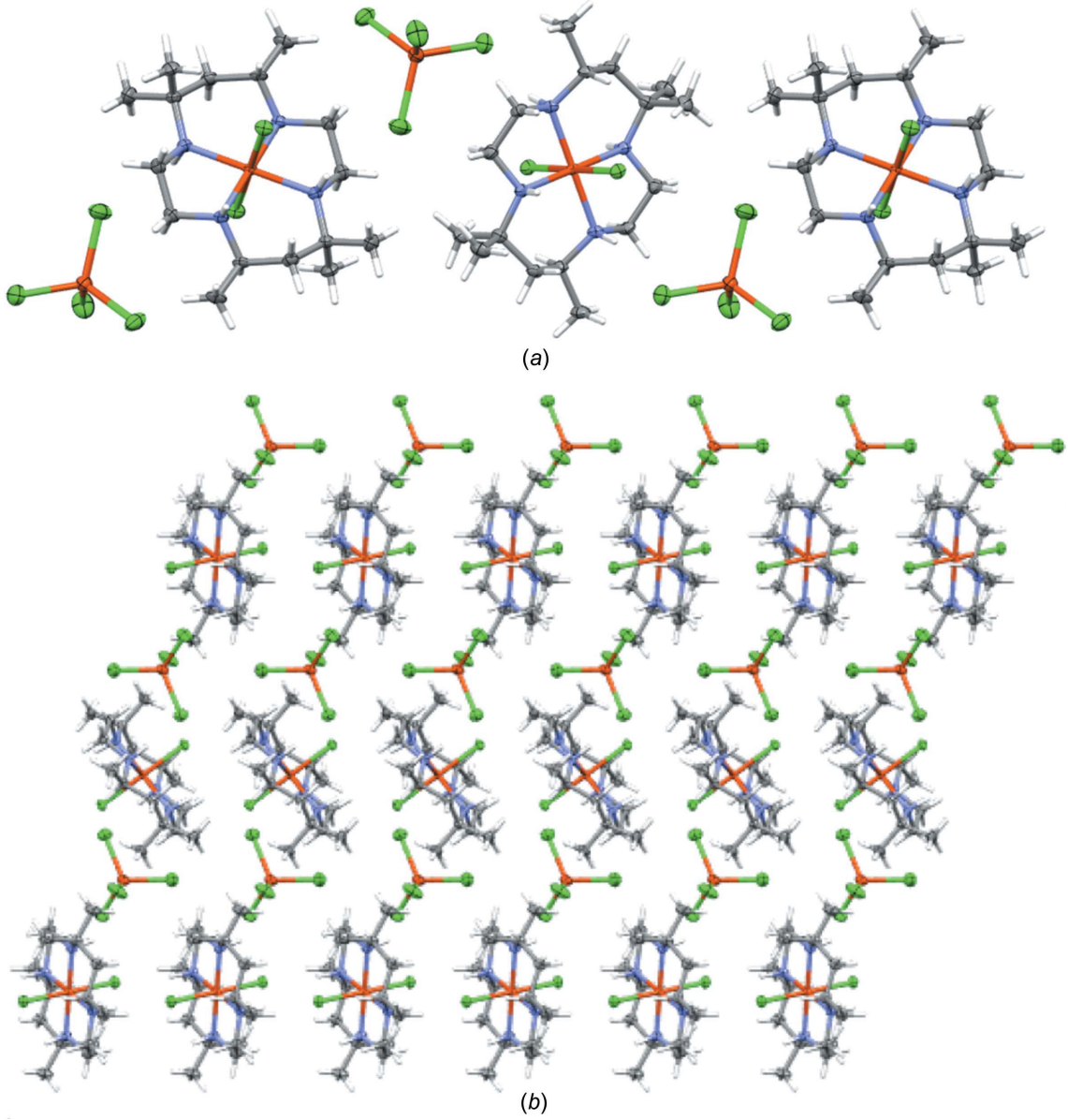

Figure 7
View of the packing of **2** along (*a*) the *a* axis and (*b*) the *c* axis, illustrating the alternating columns of cations and anions down the *a* axis.

Table 4
Hydrogen-bond geometry (Å, °) for **1**.

D—H···A	D—H	H···A	D···A	D—H···A
N1—H1···Cl2^{i}	0.86 (2)	2.78 (2)	3.5467 (15)	150 (2)
N2—H2···Cl2	0.84 (2)	2.47 (2)	3.2971 (16)	168 (2)

Symmetry code: (i) $x, y+\frac{1}{2}, z+\frac{1}{2}$.

by glide planes. Hydrogen-bonding interactions appear to be limited to species of the same enantiomer, leading to 'layers' of packing which may be distinguished when viewed along the *b* or *c* axes, with hydrogen bonding within, but not between, each layer (see Figs. 5*a* and 5*b*). Hydrogen-bonding interactions exist between the chloride counter-anions and the amine H atoms of **1** (Fig. 6). For a given formula unit, there exist two independent amine groups and one chloride counter-anion within the asymmetric unit. Both amine groups take part in hydrogen bonding, one with the nearest chloride counter-anion and the other with a counter-anion from a neighboring moiety. The closer of these interactions (Cl2···H2 = 2.47 Å) seems to determine the location of the counter-anion relative to the cation, locating the chloride between two amine functional groups (one independent and the other symmetry created). The weaker hydrogen–chloride interaction (Cl1···H1 = 2.78 Å) instead determines the packing of these moieties within the layers. Thus, the moieties are oriented in such a fashion as to minimize the distance between the

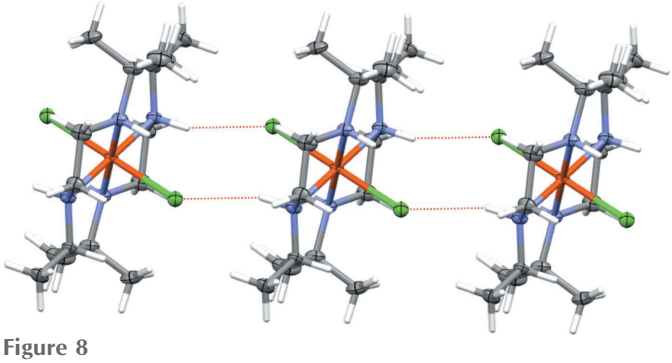

Figure 8
Hydrogen-bonding interactions between cationic fragments in **2** (N2—H2···Cl1^{ii} and N3—H3···Cl2^{iii}; Table 5). Hydrogen bonds are shown as red dotted lines.

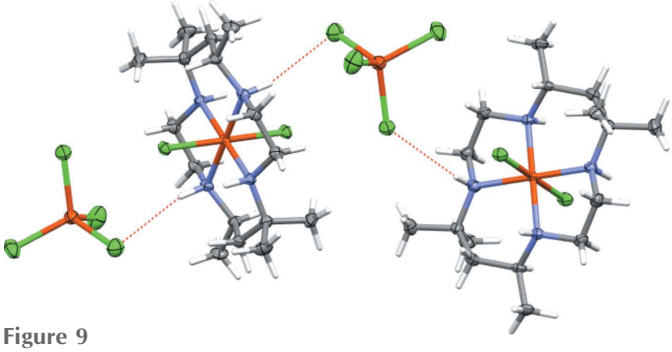

Figure 9
Hydrogen-bonding interactions between the anions and cations of **2** (N1—H1···Cl6^{i} and N4—H4···Cl4; Table 5). Hydrogen bonds are shown in red dotted lines.

Table 5
Hydrogen-bond geometry (Å, °) for **2**.

D—H···A	D—H	H···A	D···A	D—H···A
N1—H1···Cl6^{i}	0.88 (2)	2.99 (2)	3.686 (2)	138 (2)
N2—H2···Cl1^{ii}	0.87 (2)	2.66 (2)	3.487 (2)	158 (2)
N3—H3···Cl2^{iii}	0.86 (2)	2.85 (2)	3.5519 (19)	139 (2)
N4—H4···Cl4	0.87 (2)	2.87 (2)	3.699 (2)	160 (2)

Symmetry codes: (i) $-x, -y+2, -z$; (ii) $x-1, y, z$; (iii) $-x, -y+1, -z$.

outward-facing amine H atoms and the counter-anions of neighboring moieties. No significant hydrogen bonding is observed between the layers of packing. Instead, interactions between these layers appear to be governed by steric factors involving the methyl groups of the macrocycle; see Table 4 for the hydrogen-bond parameters and symmetry operators of **1**.

Compound **2** packs in a series of alternating columns of cations and anions down the *a* axis (Figs. 7*a* and 7*b*). All the amine H atoms take part in hydrogen-bonding interactions with Cl atoms. Two amine groups oriented across the macrocycle from each other (*i.e.* at the 4- and 11-positions of the macrocycle) take part in hydrogen bonding with the cationic fragments above and below the moiety under consideration (Fig. 8). The remaining amine H atoms (*i.e.* at the 1- and 8-positions) interact with two $[FeCl_4]^-$ anions *via* hydrogen bonding. Likewise, each anion participates in hydrogen-bonding interactions with two separate cations (Fig. 9). Additionally, it appears that there may be some weak interactions between the remaining Cl atoms of the anion and C—H groups; however, these would be substantially weaker than the true hydrogen bonds involving the macrocyclic amine groups. Thus, the structure consists of columns of cations tethered to one another *via* hydrogen bonds, while other hydrogen bonds serve to interconnect these columns *via* the $[FeCl_4]^-$ anions; see Table 5 for the hydrogen-bond parameters of **2**.

Funding information

Funding for this research was provided by: National Science Foundation, Directorate for Mathematical and Physical Sciences (award No. CHE1764347 to TR, for research; award No. CHE1625543 to TR and MZ, for the diffractometers).

References

Bosnich, B., Poon, C. K. & Tobe, M. L. (1965). *Inorg. Chem.* **4**, 1102–1108.
Bruker (2018). *APEX* and *SAINT*. Bruker AXS Inc., Madison, Wisconsin, USA.
Cao, Z., Fanwick, P. E., Forrest, W. P., Gao, Y. & Ren, T. (2013). *Organometallics*, **32**, 4684–4689.
Cao, Z., Forrest, W. P., Gao, Y., Fanwick, P. E. & Ren, T. (2012). *Organometallics*, **31**, 6199–6206.
Cook, T. D., Natoli, S. N., Fanwick, P. E. & Ren, T. (2015). *Organometallics*, **34**, 686–689.
Cook, T. D., Natoli, S. N., Fanwick, P. E. & Ren, T. (2016). *Organometallics*, **35**, 1329–1338.
Curtis, N. F. (1979). *Structural Aspects*, in *Coordination Chemistry of Macrocyclic Compounds*, edited by G. A. Melson. New York: Plenum Press.

Dei, A., Gatteschi, D. & Pardi, L. (1993). *Inorg. Chem.* **32**, 1389–1395.
Guilard, R., Siri, O., Tabard, A., Broeker, G., Richard, P., Nurco, D. J. & Smith, K. M. (1997). *J. Chem. Soc. Dalton Trans.* pp. 3459–3463.
Hay, R. W., Lawrance, G. A. & Curtis, N. F. (1975). *J. Chem. Soc. Perkin Trans. 1*, pp. 591–593.
House, D. A., Hay, R. W. & Akbar Ali, M. (1983). *Inorg. Chim. Acta*, **72**, 239–245.
Hübschle, C. B., Sheldrick, G. M. & Dittrich, B. (2011). *J. Appl. Cryst.* **44**, 1281–1284.
Judkins, E. C., Tyler, S. F., Zeller, M., Fanwick, P. E. & Ren, T. (2017). *Eur. J. Inorg. Chem.* **2017**, 4068–4076.
Krause, L., Herbst-Irmer, R., Sheldrick, G. M. & Stalke, D. (2015). *J. Appl. Cryst.* **48**, 3–10.
Macrae, C. F., Bruno, I. J., Chisholm, J. A., Edgington, P. R., McCabe, P., Pidcock, E., Rodriguez-Monge, L., Taylor, R., van de Streek, J. & Wood, P. A. (2008). *J. Appl. Cryst.* **41**, 466–470.
Natoli, S. N., Azbell, T. J., Fanwick, P. E., Zeller, M. & Ren, T. (2016). *Organometallics*, **35**, 3594–3603.
Natoli, S. N., Cook, T. D., Abraham, T. R., Kiernicki, J. J., Fanwick, P. E. & Ren, T. (2015). *Organometallics*, **34**, 5207–5209.
Natoli, S. N., Zeller, M. & Ren, T. (2019). *Organometallics*, **38**, 2758–2769.
Neumann, T., Weyhermüller, T., Schucht, H. & Wieghardt, K. (2003). *CSD Communication* (CCDC deposition No. 210558). CCDC, Cambridge, England.
Nishijo, J., Judai, K. & Nishi, N. (2011). *Inorg. Chem.* **50**, 3464–3470.
Ren, T. (2016). *Chem. Commun.* **52**, 3271–3279.
Sheldrick, G. M. (2008). *Acta Cryst.* A**64**, 112–122.
Sheldrick, G. M. (2015). *Acta Cryst.* C**71**, 3–8.
Tyler, S. F., Judkins, E. C., Song, Y., Cao, F., McMillin, D. R., Fanwick, P. E. & Ren, T. (2016). *Inorg. Chem.* **55**, 8736–8743.
Westrip, S. P. (2010). *J. Appl. Cryst.* **43**, 920–925.

supporting information

Acta Cryst. (2019). C**75**, 1509-1516 [https://doi.org/10.1107/S2053229619013925]

Crystal structures of two (5,5,7,12,12,14-hexamethyl-1,4,8,11-tetraazacyclotetradecane)iron(III) complexes

Reese A. Clendening, Matthias Zeller and Tong Ren

Computing details

For both structures, data collection: *APEX3* (Bruker, 2018); cell refinement: *SAINT* (Bruker, 2018); data reduction: *SAINT* (Bruker, 2018); program(s) used to solve structure: SHELXM (Sheldrick, 2008); program(s) used to refine structure: *SHELXL2018* (Sheldrick, 2015) and SHELXLE (Hübschle *et al.*, 2011); molecular graphics: *Mercury* (Macrae *et al.*, 2008); software used to prepare material for publication: *publCIF* (Westrip, 2010).

Dichlorido(5,5,7,12,12,14-hexamethyl-1,4,8,11-tetraazacyclotetradecane)iron(III) chloride (1)

Crystal data

$[FeCl_2(C_{16}H_{36}N_4)]Cl$
M_r = 446.69
Orthorhombic, *Fdd*2
a = 34.5658 (16) Å
b = 9.3832 (4) Å
c = 12.5209 (6) Å
V = 4061.0 (3) Å^3
Z = 8
$F(000)$ = 1896
D_x = 1.461 Mg m^{-3}
Mo $K\alpha$ radiation, λ = 0.71073 Å
Cell parameters from 9904 reflections
θ = 2.8–34.4°
μ = 1.14 mm^{-1}
T = 150 K
Plate, yellow
0.18 × 0.17 × 0.05 mm

Data collection

Bruker D8 Quest CMOS diffractometer
Radiation source: sealed tube X-ray source
Triumph curved graphite crystal monochromator
Detector resolution: 10.4167 pixels mm^{-1}
ω and phi scans
Absorption correction: multi-scan (Krause *et al.*, 2015)
T_{min} = 0.595, T_{max} = 0.747
17097 measured reflections
4166 independent reflections
3897 reflections with $I > 2\sigma(I)$
R_{int} = 0.042
θ_{max} = 34.4°, θ_{min} = 2.8°
h = −54→54
k = −14→14
l = −17→19

Refinement

Refinement on F^2
Least-squares matrix: full
$R[F^2 > 2\sigma(F^2)]$ = 0.025
$wR(F^2)$ = 0.064
S = 1.06
4166 reflections
120 parameters
2 restraints
Primary atom site location: structure-invariant direct methods
Secondary atom site location: difference Fourier map
Hydrogen site location: mixed
H atoms treated by a mixture of independent and constrained refinement
$w = 1/[\sigma^2(F_o^2) + (0.0327P)^2]$ where $P = (F_o^2 + 2F_c^2)/3$
$(\Delta/\sigma)_{max}$ = 0.030
$\Delta\rho_{max}$ = 0.86 e Å^{-3}
$\Delta\rho_{min}$ = −0.58 e Å^{-3}

Absolute structure: Refined as an inversion twin Absolute structure parameter: 0.004 (13)

Special details

Geometry. All esds (except the esd in the dihedral angle between two l.s. planes) are estimated using the full covariance matrix. The cell esds are taken into account individually in the estimation of esds in distances, angles and torsion angles; correlations between esds in cell parameters are only used when they are defined by crystal symmetry. An approximate (isotropic) treatment of cell esds is used for estimating esds involving l.s. planes.

Refinement. Refined as a 2-component inversion twin

Fractional atomic coordinates and isotropic or equivalent isotropic displacement parameters (Å²)

	x	*y*	*z*	U_{iso}*/U_{eq}
Fe1	0.000000	0.500000	0.47177 (2)	0.01024 (7)
Cl1	0.04066 (2)	0.59399 (4)	0.59972 (4)	0.01780 (8)
N1	−0.01980 (4)	0.71984 (15)	0.43765 (12)	0.0120 (2)
H1	−0.0100 (7)	0.760 (3)	0.493 (2)	0.014*
N2	0.04360 (3)	0.55678 (13)	0.35009 (12)	0.0113 (2)
H2	0.0352 (7)	0.533 (3)	0.2897 (19)	0.014*
C1	0.00232 (4)	0.76806 (17)	0.34277 (15)	0.0139 (3)
H1A	0.002287	0.873496	0.339879	0.017*
H1AB	−0.010308	0.732065	0.277130	0.017*
C2	0.04357 (4)	0.71467 (16)	0.34726 (16)	0.0141 (3)
H2A	0.057976	0.748405	0.283775	0.017*
H2AB	0.056538	0.752492	0.411806	0.017*
C3	0.08320 (5)	0.49628 (15)	0.36508 (14)	0.0130 (3)
H3	0.091517	0.515461	0.440218	0.016*
C4	0.08278 (4)	0.33465 (16)	0.34788 (15)	0.0145 (3)
H4A	0.070712	0.315941	0.277559	0.017*
H4AB	0.109969	0.302072	0.343351	0.017*
C5	0.06217 (5)	0.24162 (15)	0.43060 (14)	0.0129 (3)
C6	0.11327 (5)	0.5615 (2)	0.28966 (16)	0.0193 (3)
H6A	0.105473	0.544654	0.215473	0.029*
H6B	0.138525	0.517310	0.302598	0.029*
H6C	0.115042	0.664296	0.302647	0.029*
C7	0.07963 (5)	0.25789 (19)	0.54183 (17)	0.0183 (3)
H7A	0.107197	0.233676	0.539414	0.027*
H7B	0.066338	0.193831	0.591581	0.027*
H7C	0.076579	0.356608	0.565959	0.027*
C8	0.06705 (5)	0.08418 (18)	0.39781 (15)	0.0175 (3)
H8A	0.059364	0.072337	0.322999	0.026*
H8B	0.050716	0.024097	0.443246	0.026*
H8C	0.094184	0.056091	0.406353	0.026*
Cl2	0.000000	0.500000	0.11978 (5)	0.02101 (12)

Atomic displacement parameters (Å²)

	U^{11}	U^{22}	U^{33}	U^{12}	U^{13}	U^{23}
Fe1	0.01000 (12)	0.01121 (12)	0.00952 (13)	0.00018 (11)	0.000	0.000
Cl1	0.01758 (16)	0.02242 (18)	0.01340 (16)	−0.00021 (13)	−0.00299 (14)	−0.00439 (15)

N1	0.0112 (5)	0.0134 (5)	0.0114 (6)	0.0009 (4)	−0.0002 (4)	−0.0011 (4)
N2	0.0108 (5)	0.0115 (5)	0.0116 (5)	0.0001 (4)	−0.0005 (5)	0.0003 (5)
C1	0.0136 (6)	0.0120 (6)	0.0161 (8)	0.0018 (4)	0.0020 (6)	0.0024 (5)
C2	0.0130 (6)	0.0112 (6)	0.0180 (7)	−0.0008 (5)	0.0010 (6)	0.0013 (5)
C3	0.0101 (6)	0.0151 (6)	0.0138 (7)	0.0003 (5)	0.0006 (5)	0.0018 (5)
C4	0.0126 (6)	0.0150 (6)	0.0159 (7)	0.0020 (5)	0.0030 (6)	0.0006 (6)
C5	0.0115 (6)	0.0134 (6)	0.0137 (7)	0.0028 (5)	0.0006 (5)	0.0014 (5)
C6	0.0142 (7)	0.0194 (7)	0.0244 (8)	0.0010 (6)	0.0057 (6)	0.0051 (6)
C7	0.0181 (7)	0.0202 (7)	0.0165 (7)	0.0021 (6)	−0.0042 (7)	0.0018 (6)
C8	0.0175 (7)	0.0140 (6)	0.0210 (8)	0.0050 (6)	0.0017 (6)	0.0008 (6)
Cl2	0.0267 (3)	0.0226 (3)	0.0137 (3)	−0.0070 (2)	0.000	0.000

Geometric parameters (Å, º)

Fe1—N2	2.2081 (14)	C3—C4	1.532 (2)
Fe1—N2^{i}	2.2081 (14)	C3—C6	1.532 (2)
Fe1—N1	2.2149 (14)	C3—H3	1.0000
Fe1—N1^{i}	2.2150 (14)	C4—C5	1.530 (2)
Fe1—Cl1	2.3065 (5)	C4—H4A	0.9900
Fe1—Cl1^{i}	2.3066 (5)	C4—H4AB	0.9900
N1—C1	1.483 (2)	C5—C7	1.526 (3)
N1—C5^{i}	1.511 (2)	C5—C8	1.543 (2)
N1—H1	0.86 (2)	C6—H6A	0.9800
N2—C2	1.4819 (19)	C6—H6B	0.9800
N2—C3	1.494 (2)	C6—H6C	0.9800
N2—H2	0.84 (2)	C7—H7A	0.9800
C1—C2	1.512 (2)	C7—H7B	0.9800
C1—H1A	0.9900	C7—H7C	0.9800
C1—H1AB	0.9900	C8—H8A	0.9800
C2—H2A	0.9900	C8—H8B	0.9800
C2—H2AB	0.9900	C8—H8C	0.9800
N2—Fe1—N2^{i}	92.75 (7)	H2A—C2—H2AB	108.2
N2—Fe1—N1	81.55 (5)	N2—C3—C4	110.47 (12)
N2^{i}—Fe1—N1	83.15 (5)	N2—C3—C6	113.11 (13)
N2—Fe1—N1^{i}	83.15 (5)	C4—C3—C6	108.39 (14)
N2^{i}—Fe1—N1^{i}	81.55 (5)	N2—C3—H3	108.2
N1—Fe1—N1^{i}	157.76 (8)	C4—C3—H3	108.2
N2—Fe1—Cl1	88.35 (4)	C6—C3—H3	108.2
N2^{i}—Fe1—Cl1	170.88 (3)	C5—C4—C3	118.29 (14)
N1—Fe1—Cl1	88.06 (4)	C5—C4—H4A	107.7
N1^{i}—Fe1—Cl1	107.56 (4)	C3—C4—H4A	107.7
N2—Fe1—Cl1^{i}	170.88 (3)	C5—C4—H4AB	107.7
N2^{i}—Fe1—Cl1^{i}	88.34 (4)	C3—C4—H4AB	107.7
N1—Fe1—Cl1^{i}	107.56 (4)	H4A—C4—H4AB	107.1
N1^{i}—Fe1—Cl1^{i}	88.06 (4)	N1^{i}—C5—C7	107.84 (14)
Cl1—Fe1—Cl1^{i}	92.01 (2)	N1^{i}—C5—C4	110.74 (12)
C1—N1—C5^{i}	112.32 (13)	C7—C5—C4	112.12 (14)

C1—N1—Fe1	106.22 (9)	N1^{i}—C5—C8	110.54 (13)
C5^{i}—N1—Fe1	122.25 (10)	C7—C5—C8	107.19 (13)
C1—N1—H1	108.0 (17)	C4—C5—C8	108.37 (14)
C5^{i}—N1—H1	109.0 (16)	C3—C6—H6A	109.5
Fe1—N1—H1	97.5 (17)	C3—C6—H6B	109.5
C2—N2—C3	112.55 (11)	H6A—C6—H6B	109.5
C2—N2—Fe1	104.91 (10)	C3—C6—H6C	109.5
C3—N2—Fe1	116.56 (10)	H6A—C6—H6C	109.5
C2—N2—H2	104.3 (17)	H6B—C6—H6C	109.5
C3—N2—H2	109.0 (16)	C5—C7—H7A	109.5
Fe1—N2—H2	108.8 (17)	C5—C7—H7B	109.5
N1—C1—C2	110.80 (14)	H7A—C7—H7B	109.5
N1—C1—H1A	109.5	C5—C7—H7C	109.5
C2—C1—H1A	109.5	H7A—C7—H7C	109.5
N1—C1—H1AB	109.5	H7B—C7—H7C	109.5
C2—C1—H1AB	109.5	C5—C8—H8A	109.5
H1A—C1—H1AB	108.1	C5—C8—H8B	109.5
N2—C2—C1	109.43 (12)	H8A—C8—H8B	109.5
N2—C2—H2A	109.8	C5—C8—H8C	109.5
C1—C2—H2A	109.8	H8A—C8—H8C	109.5
N2—C2—H2AB	109.8	H8B—C8—H8C	109.5
C1—C2—H2AB	109.8		

C5^{i}—N1—C1—C2	−174.18 (13)	C2—N2—C3—C6	−48.38 (19)
Fe1—N1—C1—C2	−38.12 (15)	Fe1—N2—C3—C6	−169.64 (11)
C3—N2—C2—C1	−174.53 (14)	N2—C3—C4—C5	−69.37 (19)
Fe1—N2—C2—C1	−46.83 (16)	C6—C3—C4—C5	166.19 (14)
N1—C1—C2—N2	59.91 (19)	C3—C4—C5—N1^{i}	60.64 (19)
C2—N2—C3—C4	−170.07 (15)	C3—C4—C5—C7	−59.86 (18)
Fe1—N2—C3—C4	68.67 (15)	C3—C4—C5—C8	−177.95 (14)

Symmetry code: (i) −*x*, −*y*+1, *z*.

Hydrogen-bond geometry (Å, º)

D—H···*A*	*D*—H	H···*A*	*D*···*A*	*D*—H···*A*
N1—H1···Cl2^{ii}	0.86 (2)	2.78 (2)	3.5467 (15)	150 (2)
N2—H2···Cl2	0.84 (2)	2.47 (2)	3.2971 (16)	168 (2)

Symmetry code: (ii) *x*, *y*+1/2, *z*+1/2.

Dichlorido(5,5,7,12,12,14-hexamethyl-1,4,8,11-tetraazacyclotetradecane)iron(III) tetrachloridoferrate (2)

Crystal data

$[FeCl_2(C_{16}H_{36}N_4)][FeCl_4]$
M_r = 608.89
Monoclinic, $P2_1/c$
a = 6.5569 (2) Å
b = 19.1663 (5) Å
c = 20.2946 (5) Å
β = 95.3558 (15)°
V = 2539.32 (12) Å^3
Z = 4
$F(000)$ = 1256
D_x = 1.593 Mg m^{-3}
Cu $K\alpha$ radiation, λ = 1.54178 Å
Cell parameters from 9909 reflections
θ = 3.2–80.2°

μ = 15.06 mm^{-1}
T = 150 K

Plate, orange
0.18 × 0.09 × 0.05 mm

Data collection

Bruker AXS D8 Quest CMOS diffractometer
Radiation source: I-mu-S microsource X-ray tube
Laterally graded multilayer (Goebel) mirror monochromator
Detector resolution: 7.4074 pixels mm^{-1}
ω and phi scans
Absorption correction: multi-scan (Krause *et al.*, 2015)

T_{min} = 0.426, T_{max} = 0.754
26483 measured reflections
5481 independent reflections
4930 reflections with $I > 2\sigma(I)$
R_{int} = 0.044
θ_{max} = 81.3°, θ_{min} = 3.2°
h = −8→6
k = −24→24
l = −25→25

Refinement

Refinement on F^2
Least-squares matrix: full
$R[F^2 > 2\sigma(F^2)]$ = 0.032
$wR(F^2)$ = 0.086
S = 1.11
5481 reflections
274 parameters
6 restraints
Primary atom site location: structure-invariant direct methods
Secondary atom site location: difference Fourier map
Hydrogen site location: mixed
H atoms treated by a mixture of independent and constrained refinement
$w = 1/[\sigma^2(F_o^2) + (0.0331P)^2 + 2.0722P]$ where $P = (F_o^2 + 2F_c^2)/3$
$(\Delta/\sigma)_{max}$ = 0.001
$\Delta\rho_{max}$ = 0.76 e Å^{-3}
$\Delta\rho_{min}$ = −0.57 e Å^{-3}

Special details

Geometry. All esds (except the esd in the dihedral angle between two l.s. planes) are estimated using the full covariance matrix. The cell esds are taken into account individually in the estimation of esds in distances, angles and torsion angles; correlations between esds in cell parameters are only used when they are defined by crystal symmetry. An approximate (isotropic) treatment of cell esds is used for estimating esds involving l.s. planes.

Fractional atomic coordinates and isotropic or equivalent isotropic displacement parameters (Å^2)

	x	y	z	U_{iso}*/U_{eq}
C1	−0.0492 (4)	1.11813 (12)	0.10684 (11)	0.0232 (5)
C2	−0.1633 (5)	1.18787 (14)	0.10898 (14)	0.0346 (6)
H2A	−0.084339	1.224426	0.089129	0.052*
H2B	−0.180296	1.200042	0.155047	0.052*
H2C	−0.298274	1.183688	0.084114	0.052*
C3	0.1555 (4)	1.12327 (14)	0.14890 (12)	0.0297 (5)
H3A	0.231959	1.079690	0.145364	0.045*
H3B	0.131237	1.131251	0.195216	0.045*
H3C	0.234986	1.162156	0.133134	0.045*
C4	−0.1897 (4)	1.06314 (13)	0.13413 (11)	0.0243 (5)
H4A	−0.215710	1.077966	0.179321	0.029*
H4AB	−0.322629	1.065052	0.106727	0.029*
C5	−0.1231 (4)	0.98678 (13)	0.13820 (11)	0.0206 (4)
H5	0.027068	0.984812	0.152253	0.025*
C6	−0.2370 (4)	0.94789 (14)	0.18902 (12)	0.0280 (5)
H6A	−0.384013	0.947843	0.174889	0.042*

H6B	−0.212902	0.971097	0.232071	0.042*
H6C	−0.187189	0.899710	0.192790	0.042*
C7	−0.1294 (4)	0.87858 (12)	0.06771 (12)	0.0240 (5)
H7A	−0.238405	0.853989	0.089144	0.029*
H7AB	0.004589	0.865893	0.091186	0.029*
C8	−0.1358 (4)	0.85781 (13)	−0.00432 (12)	0.0270 (5)
H8A	−0.107160	0.807318	−0.008034	0.032*
H8AB	−0.273230	0.867329	−0.026998	0.032*
C9	0.3590 (3)	0.38600 (12)	0.09872 (11)	0.0206 (4)
C10	0.1558 (4)	0.35671 (15)	0.11853 (13)	0.0303 (5)
H10A	0.060053	0.395164	0.123661	0.045*
H10B	0.180228	0.331459	0.160515	0.045*
H10C	0.097286	0.324785	0.084078	0.045*
C11	0.5122 (4)	0.32617 (13)	0.09735 (12)	0.0265 (5)
H11A	0.453000	0.288955	0.068458	0.040*
H11B	0.543601	0.307893	0.142246	0.040*
H11C	0.638195	0.343238	0.080461	0.040*
C12	0.4309 (3)	0.44094 (12)	0.15058 (11)	0.0213 (4)
H12A	0.320651	0.476148	0.151269	0.026*
H12B	0.442905	0.417652	0.194316	0.026*
C13	0.6305 (3)	0.48006 (12)	0.14432 (11)	0.0201 (4)
H13	0.734764	0.446424	0.130329	0.024*
C14	0.7096 (4)	0.51152 (14)	0.21111 (12)	0.0288 (5)
H14A	0.841309	0.534543	0.207154	0.043*
H14B	0.727466	0.474415	0.244372	0.043*
H14C	0.610562	0.545765	0.224616	0.043*
C15	0.7680 (3)	0.58345 (12)	0.08705 (11)	0.0212 (4)
H15A	0.896328	0.556868	0.084148	0.025*
H15B	0.785607	0.613909	0.126568	0.025*
C16	0.7210 (4)	0.62701 (12)	0.02542 (11)	0.0223 (5)
H16A	0.600184	0.656944	0.030186	0.027*
H16B	0.838984	0.657466	0.018423	0.027*
N1	−0.0211 (3)	1.10117 (10)	0.03540 (9)	0.0197 (4)
H1	−0.139 (3)	1.1114 (15)	0.0134 (13)	0.024*
N2	−0.1609 (3)	0.95519 (10)	0.07070 (9)	0.0190 (4)
H2	−0.288 (3)	0.9627 (15)	0.0562 (14)	0.023*
N3	0.3209 (3)	0.42067 (10)	0.03155 (9)	0.0173 (4)
H3	0.209 (3)	0.4443 (13)	0.0335 (14)	0.021*
N4	0.5940 (3)	0.53475 (10)	0.09237 (9)	0.0177 (4)
H4	0.490 (3)	0.5576 (14)	0.1050 (13)	0.021*
Cl1	0.30936 (8)	0.97775 (3)	0.06127 (3)	0.02332 (12)
Cl2	0.21952 (7)	0.56951 (3)	0.00283 (3)	0.02014 (11)
Cl3	0.69585 (11)	0.74121 (4)	0.20082 (4)	0.04673 (19)
Cl4	0.24204 (10)	0.63793 (3)	0.18618 (3)	0.03526 (15)
Cl5	0.21825 (11)	0.82224 (4)	0.22565 (3)	0.03874 (16)
Cl6	0.32760 (14)	0.76773 (4)	0.06291 (3)	0.0490 (2)
Fe1	0.000000	1.000000	0.000000	0.01496 (11)
Fe2	0.500000	0.500000	0.000000	0.01370 (11)

Fe3	0.36770 (6)	0.74286 (2)	0.16940 (2)	0.02616 (10)

Atomic displacement parameters (Å²)

	U^{11}	U^{22}	U^{33}	U^{12}	U^{13}	U^{23}
C1	0.0344 (12)	0.0204 (11)	0.0146 (10)	0.0022 (9)	0.0018 (9)	−0.0005 (8)
C2	0.0530 (16)	0.0228 (12)	0.0283 (13)	0.0080 (12)	0.0056 (12)	−0.0043 (10)
C3	0.0409 (14)	0.0287 (13)	0.0180 (11)	−0.0060 (11)	−0.0047 (10)	−0.0043 (9)
C4	0.0296 (12)	0.0266 (12)	0.0174 (10)	0.0034 (10)	0.0063 (9)	−0.0015 (9)
C5	0.0239 (11)	0.0277 (12)	0.0108 (10)	−0.0008 (9)	0.0047 (8)	0.0011 (8)
C6	0.0313 (13)	0.0356 (14)	0.0184 (11)	−0.0014 (10)	0.0089 (9)	0.0056 (10)
C7	0.0313 (12)	0.0203 (11)	0.0212 (11)	−0.0023 (9)	0.0067 (9)	0.0041 (9)
C8	0.0381 (13)	0.0198 (11)	0.0238 (12)	−0.0056 (10)	0.0062 (10)	0.0003 (9)
C9	0.0213 (10)	0.0222 (11)	0.0184 (10)	0.0005 (9)	0.0025 (8)	0.0027 (9)
C10	0.0259 (12)	0.0367 (14)	0.0287 (13)	−0.0046 (10)	0.0046 (10)	0.0078 (11)
C11	0.0288 (12)	0.0243 (12)	0.0254 (12)	0.0061 (10)	−0.0021 (9)	0.0045 (10)
C12	0.0228 (11)	0.0261 (12)	0.0153 (10)	0.0044 (9)	0.0043 (8)	0.0019 (9)
C13	0.0210 (10)	0.0251 (11)	0.0138 (10)	0.0031 (9)	−0.0007 (8)	0.0006 (8)
C14	0.0345 (13)	0.0357 (14)	0.0149 (11)	−0.0001 (11)	−0.0038 (9)	−0.0021 (10)
C15	0.0202 (10)	0.0251 (11)	0.0179 (10)	−0.0042 (9)	−0.0003 (8)	−0.0060 (9)
C16	0.0238 (11)	0.0214 (11)	0.0213 (11)	−0.0031 (9)	0.0002 (9)	−0.0034 (9)
N1	0.0242 (9)	0.0196 (9)	0.0152 (9)	−0.0020 (7)	0.0015 (7)	−0.0014 (7)
N2	0.0217 (9)	0.0208 (9)	0.0142 (8)	0.0013 (7)	0.0009 (7)	0.0010 (7)
N3	0.0171 (8)	0.0190 (9)	0.0157 (8)	0.0023 (7)	0.0010 (7)	−0.0007 (7)
N4	0.0155 (8)	0.0233 (9)	0.0143 (8)	0.0010 (7)	0.0019 (7)	−0.0018 (7)
Cl1	0.0195 (2)	0.0293 (3)	0.0212 (3)	−0.0001 (2)	0.00196 (19)	0.0017 (2)
Cl2	0.0168 (2)	0.0231 (3)	0.0207 (2)	0.00348 (19)	0.00231 (18)	−0.00202 (19)
Cl3	0.0322 (3)	0.0408 (4)	0.0658 (5)	−0.0008 (3)	−0.0029 (3)	0.0069 (3)
Cl4	0.0390 (3)	0.0292 (3)	0.0374 (3)	−0.0048 (3)	0.0027 (3)	−0.0016 (3)
Cl5	0.0463 (4)	0.0376 (4)	0.0310 (3)	0.0097 (3)	−0.0030 (3)	−0.0129 (3)
Cl6	0.0767 (5)	0.0465 (4)	0.0243 (3)	0.0307 (4)	0.0080 (3)	0.0056 (3)
Fe1	0.0176 (2)	0.0156 (2)	0.0120 (2)	−0.00026 (17)	0.00293 (17)	0.00091 (17)
Fe2	0.0128 (2)	0.0169 (2)	0.0114 (2)	0.00094 (17)	0.00103 (16)	−0.00157 (16)
Fe3	0.0322 (2)	0.0237 (2)	0.0223 (2)	0.00353 (15)	0.00095 (15)	0.00045 (14)

Geometric parameters (Å, º)

C1—N1	1.514 (3)	C11—H11A	0.9800
C1—C3	1.525 (3)	C11—H11B	0.9800
C1—C2	1.535 (3)	C11—H11C	0.9800
C1—C4	1.536 (3)	C12—C13	1.524 (3)
C2—H2A	0.9800	C12—H12A	0.9900
C2—H2B	0.9800	C12—H12B	0.9900
C2—H2C	0.9800	C13—N4	1.490 (3)
C3—H3A	0.9800	C13—C14	1.529 (3)
C3—H3B	0.9800	C13—H13	1.0000
C3—H3C	0.9800	C14—H14A	0.9800
C4—C5	1.527 (3)	C14—H14B	0.9800

C4—H4A	0.9900	C14—H14C	0.9800
C4—H4AB	0.9900	C15—N4	1.486 (3)
C5—N2	1.497 (3)	C15—C16	1.512 (3)
C5—C6	1.523 (3)	C15—H15A	0.9900
C5—H5	1.0000	C15—H15B	0.9900
C6—H6A	0.9800	C16—N3^{ii}	1.479 (3)
C6—H6B	0.9800	C16—H16A	0.9900
C6—H6C	0.9800	C16—H16B	0.9900
C7—N2	1.485 (3)	Fe1—N1	2.0768 (19)
C7—C8	1.512 (3)	N1—H1	0.880 (19)
C7—H7A	0.9900	Fe1—N2	2.0477 (19)
C7—H7AB	0.9900	N2—H2	0.872 (19)
C8—N1^{i}	1.481 (3)	Fe2—N3	2.0595 (19)
C8—H8A	0.9900	N3—H3	0.864 (19)
C8—H8AB	0.9900	Fe2—N4	2.0301 (18)
C9—N3	1.516 (3)	N4—H4	0.869 (19)
C9—C11	1.526 (3)	Fe1—Cl1	2.3177 (5)
C9—C12	1.532 (3)	Fe2—Cl2	2.2760 (5)
C9—C10	1.534 (3)	Fe3—Cl3	2.1866 (8)
C10—H10A	0.9800	Fe3—Cl4	2.2117 (8)
C10—H10B	0.9800	Fe3—Cl5	2.1879 (7)
C10—H10C	0.9800	Fe3—Cl6	2.2048 (8)

N1—C1—C3	111.7 (2)	C13—C14—H14A	109.5
N1—C1—C2	108.51 (19)	C13—C14—H14B	109.5
C3—C1—C2	109.5 (2)	H14A—C14—H14B	109.5
N1—C1—C4	109.19 (18)	C13—C14—H14C	109.5
C3—C1—C4	111.62 (19)	H14A—C14—H14C	109.5
C2—C1—C4	106.1 (2)	H14B—C14—H14C	109.5
C1—C2—H2A	109.5	N4—C15—C16	107.96 (17)
C1—C2—H2B	109.5	N4—C15—H15A	110.1
H2A—C2—H2B	109.5	C16—C15—H15A	110.1
C1—C2—H2C	109.5	N4—C15—H15B	110.1
H2A—C2—H2C	109.5	C16—C15—H15B	110.1
H2B—C2—H2C	109.5	H15A—C15—H15B	108.4
C1—C3—H3A	109.5	N3^{ii}—C16—C15	108.31 (18)
C1—C3—H3B	109.5	N3^{ii}—C16—H16A	110.0
H3A—C3—H3B	109.5	C15—C16—H16A	110.0
C1—C3—H3C	109.5	N3^{ii}—C16—H16B	110.0
H3A—C3—H3C	109.5	C15—C16—H16B	110.0
H3B—C3—H3C	109.5	H16A—C16—H16B	108.4
C5—C4—C1	119.9 (2)	C8^{i}—N1—C1	116.44 (18)
C5—C4—H4A	107.3	C8^{i}—N1—Fe1	106.08 (14)
C1—C4—H4A	107.3	C1—N1—Fe1	123.35 (14)
C5—C4—H4AB	107.3	C8^{i}—N1—H1	106.2 (19)
C1—C4—H4AB	107.3	C1—N1—H1	104.9 (19)
H4A—C4—H4AB	106.9	Fe1—N1—H1	96.7 (19)
N2—C5—C6	111.8 (2)	C7—N2—C5	115.19 (18)

N2—C5—C4	108.42 (18)	C7—N2—Fe1	107.65 (14)
C6—C5—C4	110.5 (2)	C5—N2—Fe1	114.80 (14)
N2—C5—H5	108.7	C7—N2—H2	106.4 (19)
C6—C5—H5	108.7	C5—N2—H2	108.2 (19)
C4—C5—H5	108.7	Fe1—N2—H2	103.6 (19)
C5—C6—H6A	109.5	C16^{ii}—N3—C9	115.78 (18)
C5—C6—H6B	109.5	C16^{ii}—N3—Fe2	106.42 (14)
H6A—C6—H6B	109.5	C9—N3—Fe2	123.52 (13)
C5—C6—H6C	109.5	C16^{ii}—N3—H3	105.3 (18)
H6A—C6—H6C	109.5	C9—N3—H3	104.9 (19)
H6B—C6—H6C	109.5	Fe2—N3—H3	97.9 (18)
N2—C7—C8	107.97 (18)	C15—N4—C13	114.79 (17)
N2—C7—H7A	110.1	C15—N4—Fe2	107.94 (13)
C8—C7—H7A	110.1	C13—N4—Fe2	115.95 (14)
N2—C7—H7AB	110.1	C15—N4—H4	109.5 (18)
C8—C7—H7AB	110.1	C13—N4—H4	103.0 (19)
H7A—C7—H7AB	108.4	Fe2—N4—H4	105.0 (18)
N1^{i}—C8—C7	108.32 (19)	N2^{i}—Fe1—N2	180.0
N1^{i}—C8—H8A	110.0	N2^{i}—Fe1—N1^{i}	95.39 (8)
C7—C8—H8A	110.0	N2—Fe1—N1^{i}	84.61 (8)
N1^{i}—C8—H8AB	110.0	N2^{i}—Fe1—N1	84.61 (8)
C7—C8—H8AB	110.0	N2—Fe1—N1	95.39 (8)
H8A—C8—H8AB	108.4	N1^{i}—Fe1—N1	180.0
N3—C9—C11	111.50 (19)	N2^{i}—Fe1—Cl1	88.32 (5)
N3—C9—C12	109.32 (18)	N2—Fe1—Cl1	91.68 (5)
C11—C9—C12	111.59 (19)	N1^{i}—Fe1—Cl1	86.02 (5)
N3—C9—C10	108.78 (18)	N1—Fe1—Cl1	93.98 (5)
C11—C9—C10	108.6 (2)	N2^{i}—Fe1—Cl1^{i}	91.68 (5)
C12—C9—C10	106.90 (19)	N2—Fe1—Cl1^{i}	88.32 (5)
C9—C10—H10A	109.5	N1^{i}—Fe1—Cl1^{i}	93.98 (5)
C9—C10—H10B	109.5	N1—Fe1—Cl1^{i}	86.02 (5)
H10A—C10—H10B	109.5	Cl1—Fe1—Cl1^{i}	180.0
C9—C10—H10C	109.5	N4—Fe2—N4^{ii}	180.0
H10A—C10—H10C	109.5	N4—Fe2—N3	95.04 (7)
H10B—C10—H10C	109.5	N4^{ii}—Fe2—N3	84.97 (7)
C9—C11—H11A	109.5	N4—Fe2—N3^{ii}	84.96 (7)
C9—C11—H11B	109.5	N4^{ii}—Fe2—N3^{ii}	95.03 (7)
H11A—C11—H11B	109.5	N3—Fe2—N3^{ii}	180.0
C9—C11—H11C	109.5	N4—Fe2—Cl2	87.76 (5)
H11A—C11—H11C	109.5	N4^{ii}—Fe2—Cl2	92.23 (5)
H11B—C11—H11C	109.5	N3—Fe2—Cl2	86.49 (5)
C13—C12—C9	119.51 (19)	N3^{ii}—Fe2—Cl2	93.51 (5)
C13—C12—H12A	107.4	N4—Fe2—Cl2^{ii}	92.23 (5)
C9—C12—H12A	107.4	N4^{ii}—Fe2—Cl2^{ii}	87.77 (5)
C13—C12—H12B	107.4	N3—Fe2—Cl2^{ii}	93.51 (5)
C9—C12—H12B	107.4	N3^{ii}—Fe2—Cl2^{ii}	86.49 (5)
H12A—C12—H12B	107.0	Cl2—Fe2—Cl2^{ii}	180.0
N4—C13—C12	108.82 (17)	Cl3—Fe3—Cl5	109.53 (3)

N4—C13—C14	111.64 (19)	Cl3—Fe3—Cl6	108.24 (4)
C12—C13—C14	110.04 (19)	Cl5—Fe3—Cl6	110.05 (3)
N4—C13—H13	108.8	Cl3—Fe3—Cl4	108.22 (3)
C12—C13—H13	108.8	Cl5—Fe3—Cl4	111.14 (3)
C14—C13—H13	108.8	Cl6—Fe3—Cl4	109.60 (3)
N1—C1—C4—C5	62.5 (3)	C8—C7—N2—C5	−169.80 (19)
C3—C1—C4—C5	−61.5 (3)	C8—C7—N2—Fe1	−40.3 (2)
C2—C1—C4—C5	179.3 (2)	C6—C5—N2—C7	−50.4 (3)
C1—C4—C5—N2	−79.0 (2)	C4—C5—N2—C7	−172.44 (19)
C1—C4—C5—C6	158.1 (2)	C6—C5—N2—Fe1	−176.30 (15)
N2—C7—C8—N1^{i}	56.4 (3)	C4—C5—N2—Fe1	61.7 (2)
N3—C9—C12—C13	−62.2 (3)	C11—C9—N3—C16^{ii}	47.7 (3)
C11—C9—C12—C13	61.6 (3)	C12—C9—N3—C16^{ii}	171.61 (18)
C10—C9—C12—C13	−179.8 (2)	C10—C9—N3—C16^{ii}	−72.0 (2)
C9—C12—C13—N4	77.3 (2)	C11—C9—N3—Fe2	−86.4 (2)
C9—C12—C13—C14	−160.0 (2)	C12—C9—N3—Fe2	37.5 (2)
N4—C15—C16—N3^{ii}	−55.2 (2)	C10—C9—N3—Fe2	153.86 (16)
C3—C1—N1—C8^{i}	−46.7 (3)	C16—C15—N4—C13	170.47 (18)
C2—C1—N1—C8^{i}	74.1 (3)	C16—C15—N4—Fe2	39.5 (2)
C4—C1—N1—C8^{i}	−170.6 (2)	C12—C13—N4—C15	172.13 (18)
C3—C1—N1—Fe1	87.5 (2)	C14—C13—N4—C15	50.5 (3)
C2—C1—N1—Fe1	−151.62 (17)	C12—C13—N4—Fe2	−60.9 (2)
C4—C1—N1—Fe1	−36.4 (2)	C14—C13—N4—Fe2	177.49 (15)

Symmetry codes: (i) −*x*, −*y*+2, −*z*; (ii) −*x*+1, −*y*+1, −*z*.

Hydrogen-bond geometry (Å, º)

D—H···*A*	*D*—H	H···*A*	*D*···*A*	*D*—H···*A*
N1—H1···Cl6^{i}	0.88 (2)	2.99 (2)	3.686 (2)	138 (2)
N2—H2···Cl1^{iii}	0.87 (2)	2.66 (2)	3.487 (2)	158 (2)
N3—H3···Cl2^{iv}	0.86 (2)	2.85 (2)	3.5519 (19)	139 (2)
N4—H4···Cl4	0.87 (2)	2.87 (2)	3.699 (2)	160 (2)

Symmetry codes: (i) −*x*, −*y*+2, −*z*; (iii) *x*−1, *y*, *z*; (iv) −*x*, −*y*+1, −*z*.